GENOME-WIDE ANALYSIS OF DROUGHT STRESS INDUCED HISTONE 3 LYSINE 4 AND HISTONE 3 LYSINE 27 TRIMETHYLATION MODIFICATIONS IN WINTER WHEAT

By

CHI-PING LIAO

Bachelor of Science in Plant Pathology
National Chung-Hsing University
Taichung City, Taiwan
2008

Master of Science in Oral Biology
National Taiwan University
Taipei City, Taiwan
2010

Submitted to the Faculty of the
Graduate College of the
Oklahoma State University
in partial fulfillment of
the requirements for
the Degree of
MASTER OF SCIENCE
July, 2020

GENOME-WIDE ANALYSIS OF DROUGHT STRESS INDUCED HISTONE 3 LYSINE 4 AND HISTONE 3 LYSINE 27 TRIMETHYLATION MODIFICATIONS IN WINTER WHEAT

Thesis Approved:

Dr. Donald D. Ruhl

Thesis Advisor

Dr. Charles Chen

Dr. Ramanjulu Sunkar

Name: CHI-PING LIAO

Date of Degree: JULY, 2020

Title of Study: GENOME-WIDE ANALYSIS OF DROUGHT INDUCED HISTONE 3 LYSINE 4 AND HISTONE 3 LYSINE 27 TRIMETHYLATION MODIFICATIONS IN WINTER WHEAT

Major Field: BIOCHEMISTRY AND MOLECULAR BIOLOGY

Abstract: Drought stress brings great impact on plant growth and development, that it is the most critical threat to world food security. Although drought responsive mechanisms plants have developed to tolerate drought stress are relatively well known, the studies of genome-wide histone modifications induced by drought or other abiotic stresses is still fragmentary. In this study, I used whole-genome ChIP-seq to study genome-wide active histone mark, histone H3 lysine 4 trimethylation (H3K4me3), and repressive histone mark, histone H3 lysine 27 trimethylation (H3K27me3) patterns in winter wheat under drought stress. I found that although similar patterns of chromosomal and genomic distributions in both WW and DT were seen, the number of genes modified by H3K4me3 mark was increased and by H3K27me3 mark was reduced under drought condition. In addition, a good portion of genes was newly modified after drought treatment, especially for H3K4me3 modification. About 43% of DT H3K4me3 marked genes were unique to drought condition, and over half of these drought-specific genes were significantly enriched with H3K4me3 in DT. Surprisingly, I identified 3,819 bivalent genes in DT, and the bivalency of over 70% of these bivalent genes was established upon water deficit. Interestingly, these newly formed bivalent genes in DT were established by depleting the repressive marks and obtaining the active marks, whereas the levels of bivalency did not change in the bivalent genes which were common in WW and DT. These results suggested that drought stress induced H3K4me3 modifications and reduced the modifications of H3K27me3, and further to enhance bivalency during drought treatment in winter wheat.

TABLE OF CONTENTS

LIST OF TABLES

Table Page

LIST OF FIGURES

Figure Page

CHAPTER I

INTRODUCTION

1.1 Wheat production in Oklahoma

Bread wheat (*Triticum aestivum L.*) is one of the most important staple crops in the world. The special weather condition in Oklahoma makes winter wheat a natural adapted crop grown in the plain great area. The limited and uncertain distribution of rainfall in the region is unfavorable for most crop production. However, the greater water content in soil at seeding time, the less dependent for winter wheat relies on rainfall while growing. Therefore, make a forecast at seeding time increases the chance of success in growing winter wheat (Chilcott and Cole, 1917). Winter wheat also requires a period of low temperature to trigger the transition from vegetative to reproductive development, which is well adapted in middle and southern Great Plains of the United States representing more than 75% of wheat production. Winter wheat is the largest cash crop in Oklahoma. In 2018 – 2019 growing season, more than 4.4 million acres of land were planted with wheat, and 110 million bushels of wheat were harvested (USDA-NASS, 2019). The long growth period of wheat satisfied the grazing needs of Oklahoma farmers in the winter but also exposes wheat plants to the prolonged extreme environmental stress factors, such as drought.

1.2 Drought stress in plants

1.2.1 Grain yield

Drought stress has a major impact on plant growth and development. Plant growth and development highly rely on cell division, cell differentiation, and enlargement. The scarcity of water resource alters the morphological, physiological, ecological and molecular traits of plants, affecting the quality and quantity of plant growth and potentially impairs crop yield. Wheat production for Oklahoma is dropped to 70 million bushels in 2018, which is 29% and 49% less than 2017 and 2016 productions (USDA-NASS, 2019). One of the major causes of the lower total wheat production is believed from abandonment due to drought (Marburger et al., 2018).
The growth stage, severity and duration of plants encounter water stress are crucial for grain yield. Several studies have proven that yield reductions can vary from 13% to 94% based on severity and duration of drought encountered (Farooq et al., 2009). In wheat, though kernel number and filling rate were less affected by drought after anthesis, severe drought treatment was still able to shorten the duration of kernel maturity and reduce kernel dry weight compared to mild drought treatment (Wardlaw and Willenbrink, 2000). Postanthesis drought stress but not stress severity was detrimental to grain yield (Samarah, 2005); however, in the duration of grain filling, grain yield decreased as drought stress severity increased (Samarah et al., 2009).

1.2.2 Plant-water relations

The factors in plant-water relations, including relative water content (RWC), leaf water potential, stomatal resistance, leaf temperature and canopy temperature are important characteristics in the relationships. Leaf RWC is an important and the earliest indicator of water status in plants. It reflects the balance of water supply and transpiration rate in the leaf (Lugojan and Ciulca, 2011). When plants first exposure to drought, significantly reduce leaf water potential and RWC, which lead to the stomatal closure and therefore decrease transpiration rate and concurrent with leaf temperature increased (Siddique et al., 2000; Mafakheri et al., 2010). Root growth is, therefore enhanced to obtain sufficient water uptake in response to the short-term water deficiency.

1.2.3 Drought avoidance and tolerance

With a limited duration of water stress or under a mild drought condition, plants employ drought avoidance strategies to increase water uptake and reduce water loss. The rates of water gain and loss remain balanced are mainly achieved by stomatal closure which is triggered by abscisic acid (ABA). This early drought response is sufficient to maintain plant growth and productivity. However, stomatal disclosure at this early stage of water deficits limits the entry of carbon dioxide to leaves and thus increasing the susceptibility to photo-damage. With the continued photosynthetic light reactions, the drop in the chloroplast CO_2 results in the accumulation of reactive oxygen species (ROS), causing oxidative stress to photosynthetic pigments, enzymes, membranes, DNA and other cellular components. (Lisar et al., 2016; Cruz de Carvalho, 2008). When water-deficiency persists for a long time, drought avoidance strategy is no longer sufficient for plants to avoid dehydration. Other protective mechanisms must be triggered to protect the cellular structure and provide damage repair, which is so called drought tolerance. The main mechanisms are metabolic adjustment which accumulates osmolytes and solutes (Somero, 1992) to protect proteins and maintain membrane structure of the cell, cell wall hardening that allows growth process to continue, ROS detoxification that limits the damage caused by ROS, (Verslues et al., 2006).

1.3 Chromatin regulation and immunoprecipitation

1.3.1 Histone posttranslational modifications

Histones are highly conserved nuclear proteins in eukaryotic cells throughout species. Core histone is composed as an octamer by two molecules each of H2A, H2B, H3 and H4. Core histone packages DNA by wrapping 147 bp of DNA and forms a fundamental unit of chromatin, nucleosome (Davey et al., 2002). Linear arrays of nucleosome cores are then connected by linker DNA that is associated with linker histone, H1.

The N-terminal tails of histones are subject to different histone post-translation modifications (PTMs) (Allfrey et al., 1964; Wu & Grunstein 2000; Kouzarides, 2007). Histone modification enzymes, such as histone methyltransferase (HMT) and histone acetylase (HAT), covalently modify the N-terminal tails of histones with different types of modification (Verbsky and Richards, 2001). The modification at histone tails, including methylation, acetylation, phosphorylation, ubiquitination, sumoylation etc., can change the histone-DNA interaction and cause changes to chromatin structure and DNA accessibility (Pfluger and Wagner, 2007). These modifications at amino acid residues in histone tails provide the complexity for the intricate regulation of gene expression (Kouzarides, 2007). Although not all of these chemical modifications are very well-studied for the association with gene activity, some of these alterations are well-studied and their function is highly conserved across species. For example, the H3K4me3 modification is found to be accumulated in promoter and 5' ends of coding regions, and is positively correlated to the abundance of RNA polymerase II binding and the levels of RNA transcripts in human cells (Okitsu et al., 2010; Bernstein et al., 2005) and *Arabidopsis* (Zhang et al., 2009; van Dijk et al., 2010). H3K27me3 marks are enhanced by polycomb repressive complexes, and are usually considered as repressive mark in human cells, yeasts and *Arabidopsis* (Cao et al., 2002; Basenko et al., 2015; Zhang et al., 2007). H3K9 acetylation leads to RNA polymerase stalling and promotes transcription elongation in *Drosophila* and mammalian cells (Wu and Snyder, 2008).

1.3.2 Histone posttranslational modifications under stress responses

Chromatin regulation has been known as a key factor of its involvement of plant growth and development, as well as abiotic stress. Recent studies have demonstrated that histone modifications alter chromatin configurations, which is coordinated with gene expression in response to environmental stimuli (Kim et al., 2010). H3K9 acetylation levels on the promoter and coding regions of cell wall related genes, ZmEXPB2 and ZmXET1, are enriched after salt

treatment in maize (Li et al., 2014). In addition, a global acetylation levels of histone H3K9 and H4K5 increased and corresponded to the elevated expression of histone acetyltransferases, ZmHATB and ZmGCN5 (Li et al., 2014). In Arabidopsis, heat-induced SUMOylation was decreased at H2B histone after heat stress treatment (Miller et al., 2013). Histone acetylation increased on genes in response to cold treatment including OsDREB1b in rice (Roy et al., 2014) and ZmDREB1 and ZmCOR413 in maize (Hu et al., 2011). These genes encode DREB transcription factors that are related to stress tolerance in plants (Agarwal et al., 2006). Under drought stress, different transcriptional outcomes were associated with the H3K4 methylation level in Arabidopsis. H3K4me1 enrichment was negatively correlated with transcript levels whereas H3K4me3 enriched positively correlated with drought responsive gene transcription; moreover, a broader distribution of H3K4me3 in ABA-related genes was observed in dehydration condition than in water-sufficient condition (van Dijk et al., 2010). RNA polymerase II accumulation was followed by H3K4me3, H3K23ac and H3K27ac enrichment on the coding region of drought-responsive genes, but the patterns of these modifications varied in a gene-specific manner in Arabidopsis (Kim et al., 2008).

1.3.3 Bivalent histone modifications

Bivalent domains are the genomic region where simultaneously marked by both active and repressive histone modifications (Voigt et al., 2013). Histone modification bivalency was first uncovered in embryonic stem cells; the bivalent domains allow rapid activation or silencing during cell differentiation (Bernstein et al., 2006). In a recent study, bivalent H3K4me3 and H3K27me3 modifications and nucleosome accessibility were both increased after exposure to cold stress in potato (Zeng et al., 2019). Furthermore, H3K27me3, as a repressive histone mark, on dehydration stress memory genes surprisingly rather than suppress the transition of gene activation, higher levels of transcripts were produced; it is believed that H3K27me3 collaborated with H3K4me3 dynamically in response to recurrent drought stress (Liu et al., 2014). These

findings suggest that bivalent genes can be rapidly activated or repressed in response to environmental cue (Voigt et al., 2013) and this strategy has also been found in stress memory to adapt to the recurring stress (Bäurle et al., 2020).

1.3.4 Techniques and technology to study PTMs

Chromatin immunoprecipitation (ChIP) is a technique for analyzing protein-DNA interactions within cells. This technique can use selected antibody specific to the target proteins or nucleosomes, to enrich the protein- or nucleosome-DNA complex. The immunoprecipitated DNA fragments can further be identified by quantitative polymerase chain reaction (q-PCR) or hybridization to a microarray, so-called ChIP-chip (Ren et al., 2000). Due to the rapid progress in next generation sequencing (NGS), chromatin immunoprecipitation followed by high-throughput DNA sequencing (ChIP-seq) has become a widely used approach to study genome-wide profiling of protein-DNA interactions since it was first introduced in 2007 (Johnson et at., 2007; Barski et at., 2007). Although both ChIP-seq and ChIP-chip are techniques to map a genome-scale protein-DNA binding sites, ChIP-seq significantly advances ChIP-chip in many ways. First, ChIP-seq has better base pair (bp) resolution to a single nucleotide, whereas 30-100 bp in general of ChIP-chip. Second, ChIP-seq is cost-effective and requires less amount of ChIP DNA that makes sample collection more applicable. Although some GC bias presents, ChIP-seq suffers less platform noise than ChIP-chip, which generates noise in the cross-hybridization step. Finally, the major drawback found in genome coverage of ChIP-chip is the limitation of sequence repertoire on the array, but ChIP-seq is only limited by the ability of alignment of reads to the genome (Park, 2009).

The resolution of ChIP-seq highly relies on the size of DNA fragments. The smaller the size ranges of fragments showed higher the fold enrichment of the protein-binding sites over the control regions (Fan et al., 2008). Prior to the ChIP experiment, DNA is sheared into small

fragment size of 100-500 bp in general by sonication or nuclease digestion. Given that the lack of a standardized ChIP-seq protocol, cross-linking ChIP (X-ChIP) or native ChIP (N-ChIP) are majorly used when performing immunoprecipitation (Park, 2009). X-ChIP uses formaldehyde to enhance protein-DNA interaction by covalent fixation. On the other hand, N-ChIP uses native and unfixed chromatin, thus requiring stable protein-DNA binding, such as nucleosomes (David et al., 2017). To map nucleosome positions and histone modifications, micrococcal nuclease (MNase) digestion without crosslinking is most commonly used to chromatin fragmentation. MNase digests linker DNA more efficiently than sonication, and N-ChIP-seq peaks showed better consistency between replicates and higher enrichments over X-ChIP-seq, therefore tends to increase resolution and reproducibility (Wedel and Siegel, 2017; David et al., 2017).

1.4 Research objectives

Drought stress induces changes of physiological mechanisms and genetic regulations in plants, which are important strategies to survive over drought duration. Previous studies have shown the correlations of histone modifications and stress, including drought, in several crops. Our understanding of genome-wide changes in histone distribution and posttranslational modifications under drought stress is still unclear. A series of genome-wide histone modifications in bread wheat was recently uncovered (Li et al., 2019), however, little is known about a genome-wide profiling of histone modifications associated to drought stress in wheat. Drought stress on wheat production has been a growing concern due to its impact on food insecurity and economy. In the regions like the southern Great Plain of Oklahoma of the United States, agricultural sustainability has become exceedingly vulnerable facing unprecedented water deficits. This study has examined genome-wide H3K4me3 and H3K27me3 modifications induced by dehydration in winter wheat. I hypothesized that histone modification is closely related to drought stress and histone bivalency may involve in gene regulation in response to water deficiency. The significance of the bivalent domains induced by drought in a hexaploid winter wheat was also discussed.

CHAPTER II

MATERIAL AND METHODS

2.1 Plant material and growth conditions

The bread wheat (Triticum aestivum) variety, Duster, was used in this study. Wheat seeds were germinated and grown in peat for 3 to 4 weeks under greenhouse conditions (16h light/8h dark, 20-22°C). Uniformly seedlings were transferred to 5L tree pots in a mixture of sand, vermiculite, and peat with a ratio of 4:2:1. After one week of post-transplant adaptation, plants were subjected to five-week vernalization at 4°C with 10-hour light cycle and then returned to greenhouse conditions with every-2 day-regular watering until booting stage (Fowler, 2018) where the drought treatment initiated. Water was withheld for six days in drought (DT) pots while well-watered (WW) pots were watered regularly. All pots were gravimetrically quantified water loss (Earl, 2003); fresh, turgid and dry weights of leaf samples from each plant were recorded to calculate relative water content (RWC) (Sade et al., 2014) before and after treatment. Leaves were harvested at the end of the treatment period and were frozen in liquid nitrogen for nucleus extraction.

2.2 Nucleus extraction and MNase digestion

The nucleus extraction was performed as described in Gendrel et al., 2005, with minor modifications. Briefly, frozen leaf tissues were ground to a fine powder to achieve a homogenous

tissue sample. The ground leaves were incubated at 4°C for 10 min in ice-cold extraction buffer (20 mM Tris-HCl, pH 8.0, 10 mM EDTA, 0.25 M Sucrose, 100 mM KCl, 40% Glycerol, 0.25% Triton-X-100 and 0.1% β-mercaptoethanol). After the incubation, the lysate was filtered through 70 μm (352350, BD) and then 40 μm sterile cell strainers (352340, BD). The filtrate was centrifuged at 6600 × g for 10 min. The pellet was washed three times with extraction buffer followed by centrifugation at 6600 × g for 10 min. The purified nuclei were resuspended in nuclei storage buffer (20 mM KCl, 10% Glycerol, 10 mM EDTA, 10mM PIPES, pH7.0 and 0.025% β-mercaptoethanol) and stored at -80°C until use. Nuclei were thaw on ice, then washed and resuspended in MNase buffer (50 mM Tris-HCl, pH 8.0, 0.25 M Sucrose, 5 mM $CaCl_2$). To determine MNase concentration for fragmentation, 0, 2.5×10^{-4} U, 5×10^{-4} U, 1×10^{-3} U, 2×10^{-3} U and 3×10^{-3} U of MNase (Sigma-Aldrich, St. Louis, MO, USA) were added to each titration point and incubated for 15 min at 37°C. Digestion was stopped by adding stop buffer (10 mM Tris-HCl, pH 8.0, 200 mM EDTA). The digestion was lysed in lysis buffer (20 mM Tris-HCl, pH 8.0, 50 mM EDTA, 200 mM NaCl, 1% SDS) by incubation for 30 min at 37°C in the presence of 0.02 μg/ul RNase A and 50 μg/ml Proteinase K. DNA fragments were separated by 1.6% agarose gel electrophoresis.

2.3 Chromatin immunoprecipitation

Nucleus isolation and MNase digestion were performed as described previously with minor modifications. Nuclei were digested with 2×10^{-4} U of MNase diluted in MNase buffer to obtain 150 -600 bp chromatin fragments. Digestion was then centrifuged to discard MNase digestion buffer. Chromatin was resuspended in hypotonic buffer [0.2 mM EDTA, 0.1 mM phenylmethylsulfonyl fluoride and 1X protease inhibitor cocktail (PIC), cOmpleteTM, Roche], and incubated for 10 min at 4°C. After incubation, N-ChIP incubation buffer (20 mM Tris-HCl, pH 8.0, 4 mM EDTA, 25 mM NaCl, 0.1 mM phenylmethylsulfonyl fluoride, and 1X PIC) was added. Cellular debris was pelleted by centrifuge at 16500 × g, 10 min at 4°C and the supernatant

was recovered. Immunoprecipitation was carried out by adding two microliters of anti-H3K4me3 antibody (Ab8580, Abcam, Cambridge, UK) or four microliters of anti-H3K27me3 antibody (07-449, Merk-Millipore, Billerica, MA, USA) and 0.02% or 0.01% of Tween 20 (Sigma-Aldrich, St. Louis, MO, USA) in 1150 µl of total volume, and were incubated for overnight on a rotating wheel at 4°C. Samples without antibody were used as no-antibody controls. 30 µl of protein A Dynabeads (Invitrogen, Carlsbad, CA, USA) were added to each sample. Samples with anti-H3K4me3 antibody were incubated at room temperature for 15 min or with anti-H3K27me3 antibody were incubated at 4°C on a rotating wheel. The immunoprecipitated complexes were then washed twice with N-ChIP wash buffer A (50 mM Tris-HCl, pH 8.0, 10 mM EDTA, 1% v/v IGEPAL® CA-630 (Louis, MO, USA), 75 mM NaCl), four times with N-ChIP wash buffer B (50 mM Tris-HCl, pH 8.0, 10 mM EDTA, 1% v/v IGEPAL® CA-630, 125 mM NaCl) and four times with N-ChIP wash buffer C (50 mM Tris-HCl, pH 8.0, 10 mM EDTA, 1% v/v IGEPAL® CA-630, 175 mM NaCl). Beads were then transferred to a new tube to reduce background noise and washed once with N-ChIP wash buffer C. The elution of protein-DNA complexes was done in elution buffer (20 mM Tris-HCl, pH 8.0, 5 mM EDTA, 1% SDS, 0.1 mM phenylmethylsulfonyl fluoride) at room temperature for 30 min on a rotating wheel. After beads were removed, the fractions were incubated with 50 µg/ml Proteinase K overnight at 37°C. DNA was purified by ChIP DNA Clean & ConcentratorTM (Zymo Research, Irvine, CA, USA) following manufacturer's instruction. DNA concentration was determined by Qubit 1X dsDNA HS Assay Kit (ThermoFisher Scientific, Waltham, MA, USA) and was stored at -20 ° C for ChIP-sequencing or real-time quantitative PCR (qPCR) validation. qPCR was performed on LightCycler® 96 Instrument (Roche, Diagnostics, Basel, Switzerland) to verify successful ChIP enrichment. The primer set, 1A0019, was designed to amplify the last exon of TraesCS1A01G001900 gene, which is a known H3K4me3 enriched region and 1A0910 to amplify the intergenic region between TraesCS1A01G064400 and TraesCS1A01G064500 genes, which is a known H3K27me3 enriched region in previous studies (Qi et al., 2018; Li et al.,2019).

The sequences of primer sets used in qPCR are listed in Table1. The 10 µl of PCR mixture consisted of 4.2 µl of 1:3 diluted ChIP DNA, 5 µl of iTaq Universal SYBR Green supermix (Biorad, Hercules, CA, USA), 0.4 µM each primer. The qPCR reaction settings were: 95 °C for 5 min denaturation, followed by 45 amplification cycles (94 °C for 30 s and 57 °C for 30 s, 72°C for 30 s) and melting curve of 95 °C for 15 s, 60 °C for 1 min, 95 °C for 15 s and cooling at 37 °C. Enrichments were calculated with percent of input method [100*2^(Ct (adjust input) – Ct(IP)] (Haring et al., 2007).

Table 1 Sequence of Primer sets used in qPCR

H3K4me3 primer marker
1A0019-F1
5'-CGATGCGTACGGGGACTCGT-3'
1A0019-R1
5'-GCAGAACGCCGTCAAGTTCCTG-3'
H3K27me3 primer marker
1A0910-F1
5'-CCCACCTGCTGCAACAACATTGC-3'
1A0910-R1
5'-CGTCGCCGACGAGCGTGT -3'

2.4 ChIP-seq and processing of sequencing data

The quality control of immunoprecipitated DNA, library construction, and next generation sequencing were performed by Novogene Co. Ltd. Pair-end 150-bp libraries were sequenced using NovaSeq 6000 Illumina platform. Raw data quality was verified by FastQC analysis. The raw reads were trimmed off low-quality reads (quality score ≤ 30), unsure bases, sequencing adapters, and filtered short reads (18 nt after trimming) to get clean reads on SKEWER (version 0.1.126). The clean reads were aligned on the International Wheat Genome Sequencing Consortium (IWGSC) reference sequence (version 1.0) with the BWA (versio 0.7.12). Duplicates

were labeled using SAMBLASTER. Mapping quality was calculated by MAPQ. Reads were visualized with Integrative Genomics Viewer [(IGV) Thorvaldsdóttir et al., 2013]. The bigwigCompare tool (Galaxy Version 3.3.2.0.0) in deepTools2 package (Ramírez et al.,2016) was used to normalize and compare BigWig files using log2 (IP/input) with default settings. Peak calling was done by MACS2 software (2.1.0) with default settings (Zhang et al., 2008) using the threshold q value = 0.05. Diffbind was used for differential analysis with the ratio of differential peak [reads per million (RPM) IP/input] that is larger than 2. Peak related genes were detected by PeakAnnotator_Cpp (version 1.4) for peak annotation. Peak distribution of different genomic regions was calculated by ChIPseeker (1.18.0) (Yu et al., 2015).

CHAPTER III

RESULTS

3.1 Drought physiological analysis

In order to demonstrate the drought-stress was well established, water usage of all plants was assessed by gravimetric method for simulating drought stress in our experimental model. During the 6-day drought stress treatment, pots were weighed every two days. Gravimetric loss of drought (DT) group started to increase after two days of drought treatment and was increased to approximately 11% at the end of the treatment (Figure 1a). The gravimetric loss of DT group was highly significant ($p < 0.005$) compared to the well-watered (WW) group. Relative water content stayed high (85%) in leaf tissues of WW group. In contrast, drought-stressed plants showed a significant decrease to 50% ($p < 0.01$) of RWC in leaf tissues (Figure 1b). These induced drought stress was therefore confirmed.

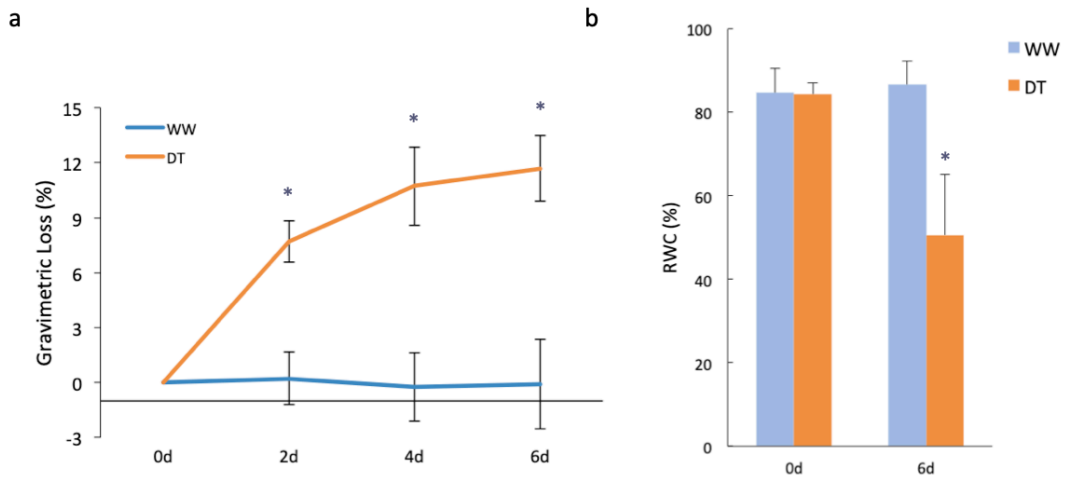

Figure 1. Physiological responses in drought-stressed wheat. Gravimetric water loss (a) and leaf relative water content (RWC) (b) of well-watered (WW) and drought treated (DT) plants. n = 4, error bars represents standard deviation, * $p < 0.01$.

3.2 Chromatin preparation and immunoprecipitation

To determine the MNase concentration required to obtain a chromatin fragment size between 150 to 600 bp, a titration series of MNase was run (0 U/µl, 2.5×10^{-4} U/µl, 5×10^{-4} U/µl, 1×10^{-3} U/µl, 2×10^{-3} U/µl and 3×10^{-3} U/µl) and imaged after agarose gel electrophoresis (Figure 2). The fragmentation pattern in lane 4 showed mono-, di-, tri- and tetra-nucleosomes after MNase digestion. With further optimization, a similar fragmentation pattern was shown in both WW and DT samples after MNase digestion. The optimal MNase concentration was determined to be 2×10^{-4} U/µl and was subsequently applied to chromatin preparation for ChIP experiment. In order to prevent a variation of the chromatin:antibody ratio, a consistent chromatin amount for each immunoprecipitation reaction was used. To do this, 20 µl of MNase digested chromatin sample was purified and quantified prior to immunoprecipitation. 3 µg of chromatin was immunoprecipitated per ChIP reaction with anti-H3K4me3 or anti-H3K27me3 antibody. 0.3 µg of chromatin samples were collected as inputs. The successful H3K4me3 and H3K27me3 histone mark enrichments were further confirmed by qPCR (Figure 3). Primer set 1A0019 and 1A0910

were designed according to the regions enriched in previous ChIP-seq studies in bread wheat (Qi et al., 2018; Li et al.,2019). Successfully H3K4me3 immunoprecipitated DNA on the last exon of TraesCS1A01G001900 gene could be amplified by the H3K4me3 marker, 1A0019, in qPCR; here the H3K27me3 marker (1A0910) was used as a negative control for H3K4me3. The H3K4me3 marker amplified the signal of H3K4me3 IP sample (28.4%) was higher than the signal amplified by using H3K27me3 marker (12.4%) (Figure 3a). Instead, H3K27me3 marker, 1A0910, was designed to amplify the intergenic region between TraesCS1A01G064400 and TraesCS1A01G064500 genes where is a known H3K27me3 enriched region. In H3K27me3 ChIP DNA, 1.56% amplification was detected when H3K27me3 marker was used and the amplification was reduced to 0.94% while using H3K4me3 marker, 1A0019, as a negative control (Figure 3b). Low background noise was confirmed by the amplification results of no antibody controls. These enrichment results were consistent to the patterns reported in previous studies (Qi et al., 2018; Li et al.,2019). 60 ng of ChIP DNA from each sample was then sent to Novogene Corp. Inc. to proceed with quality control and ChIP-seq.

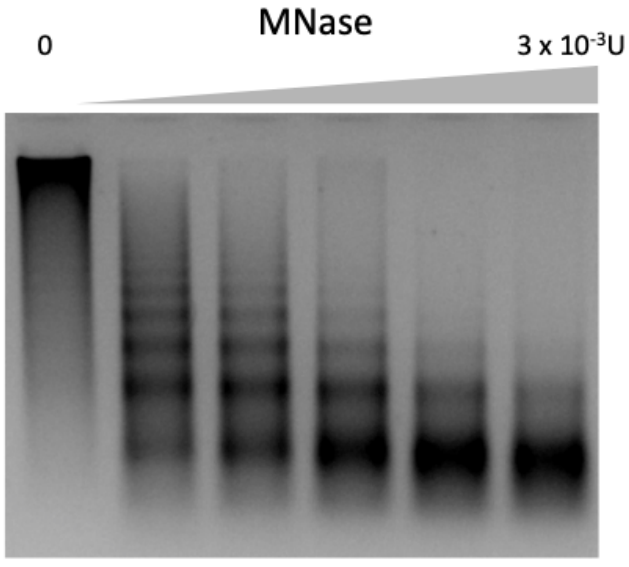

Figure 2. MNase titration experiment. From left to right lanes show chromatin digested in MNase concentrations of 0, 2.5×10^{-4} U/µl, 5×10^{-4} U/µl, 1×10^{-3} U/µl, 2×10^{-3} U/µl and 3×10^{-3} U/µl. Fragments were separated in 1.6% agarose gel electrophoresis.

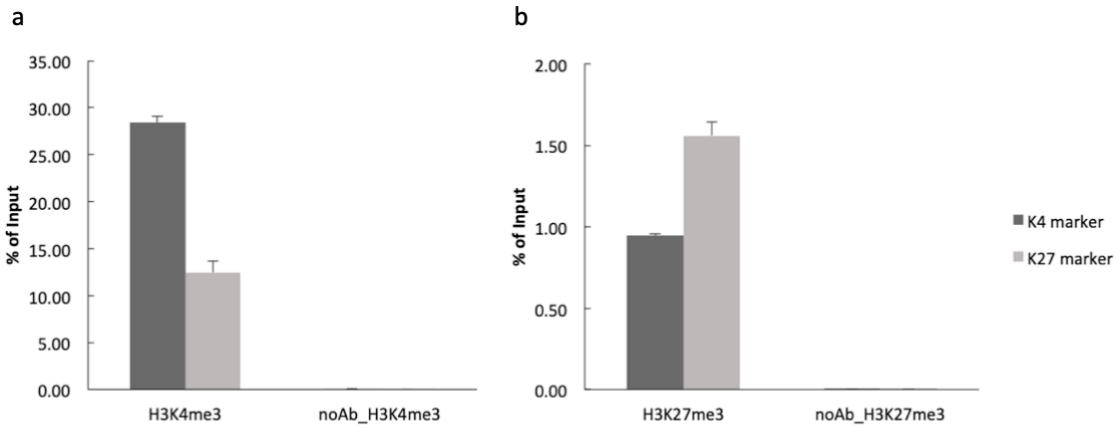

Figure 3. Histone mark verification by qPCR. Anti-H3K4me3 antibody pulled-down DNA was amplified by the 1A0019 primer set (K4 marker) (a) and anti-H3K27me3 antibody pulled-down DNA was amplified by 1A0910 primer set (K27 marker) (b). Error bars show the standard deviation of technical replicates of each DNA sample in qPCR. WW samples were used in this experiment.

3.3 Chromosomal distribution of histone modifications

H3K4me3 and H3K27me3 have been known as histone marks associated with gene activation and repression respectively. However, a systemic analysis of epigenomic features of these two histone marks in drought-stressed wheat is not well addressed. In order to understand whether and how these two gene regulatory marks are involved in response to drought systemically, specific antibodies were used to detect the regions associated with the marks on a genome-wide level. After sequencing and data trimming, I obtained over 65 million clean reads for WW H3K4me3 (WW_K4) and H3K27me3 (WW_K27) IP fractions, and over 53 million clean reads for DT IP fractions (DT_K4 and DT_K27). In well-watered samples, about 59.7 million reads of WW_K4 were mapped, 81.9% of mapped reads were uniquely mapped; 56.4 million reads of WW_K27 were mapped and 79.9% of mapped reads were uniquely mapped. In drought-stressed samples,

about 47.3 million reads of DT_K4 were mapped, 83.5% of mapped reads were uniquely mapped; 45.6 million reads of DT_K27 were mapped and 80.4% of mapped reads were uniquely mapped (Table 2).

Table 2 H3K4me3 and H3K27me3 ChIP Sequecing summary for in well-watered and drought wheat

	WW_K4	WW_K27	DT_K4	DT_K27
Total reads	68,053,294	65,121,556	54,448,244	53,423,648
Mapped reads	59,762,820	56,477,920	47,370,718	45,593,680
	87.82%	86.73%	87.00%	85.34%
Unique mapped reads	48,959,054	45,128,224	39,560,372	36,673,533
	81.92%	79.90%	83.51%	80.44%
Peak numbers	91,854	149,263	164,610	95,029
Avg. peak width (nt)	478	633	652	551
Gene numbers with peak (TSS upstream < 2kb, genes)	46,085	18,408	72,008	14,683
Gene numbers (DT peak > WW peak)[a]	-	-	30,327	6,323
Gene numbers (DT peak < WW peak)[b]	-	-	21,264	12,696
Bivalent genes (>1kb overlap)	2,204		3,819	

a DT gene number with fold change ≥ 2 peaks compared to WW.
b DT gene number with fold change ≤ 2 peaks compared to WW.

The chromosomal distribution of H3K4me3 and H3K27me3 marks were visualized by the reads of ChIP-seq normalized to the reads of input. The IGV graph showed that H3K4me3 marks were localized to interstitial and distal end regions, and H3K27me3 modifications were majorly localized to distal end regions where all were associated with high gene densities in well-watered and drought treatments (Figure 4).

3.4 Peak signatures related to genes

Peaks that represent the significant enriched regions were next detected by MACS2 peak calling software. A total of 91,854 peaks were identified in WW_K4, 149,263 peaks were identified in WW_K27. In drought fractions, 164,610 peaks and 95,029 peaks in DT_K4 and DT_K27 were identified, respectively (Table 2). The peak distribution of histone marks surrounding the genes was then analyzed (Figure 5). In H3K4me3 IP fractions, over half of peaks corresponded to promoter regions, which were defined within 2kb upstream of transcription start site (TSS) in

both conditions. The proportion of the peaks under well-watered is similar to drought-stressed (WW is about 57%, DT is about 55%).

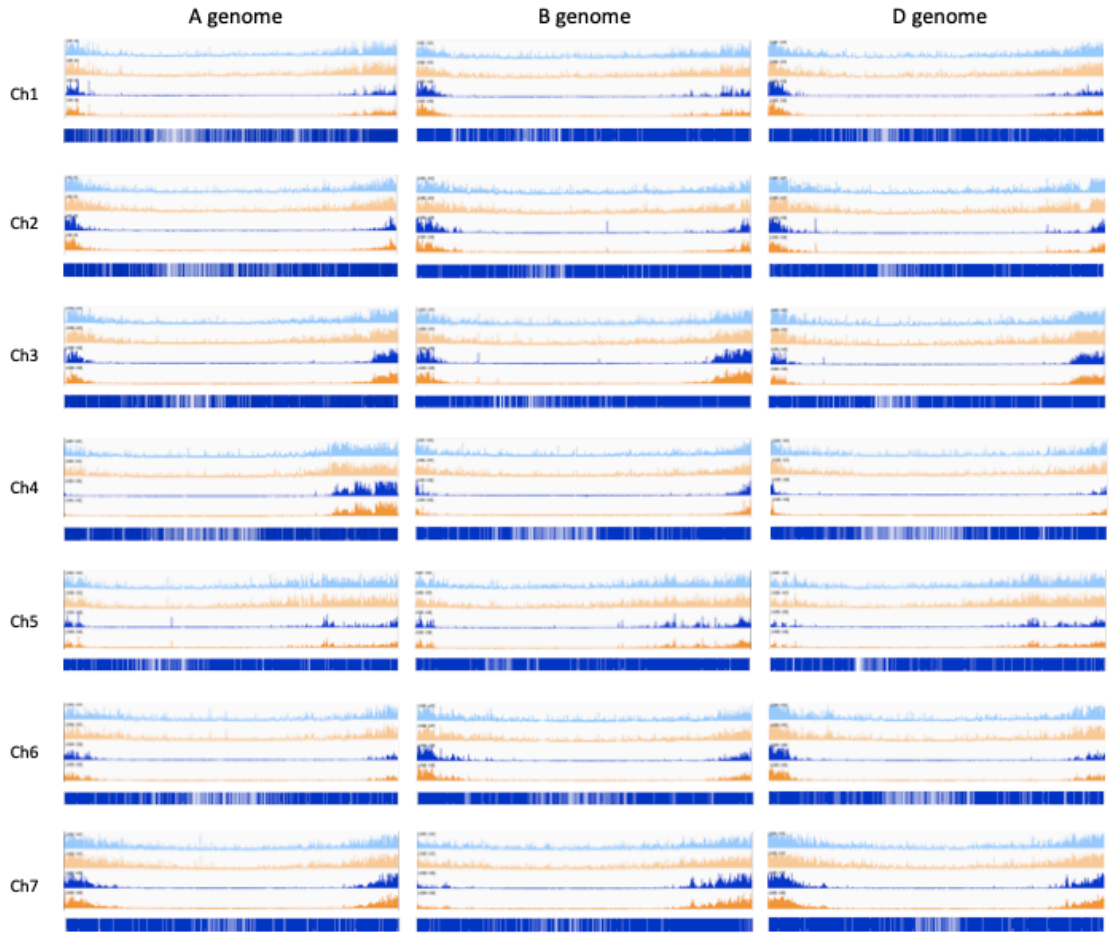

Figure 4. Visualization of chromatin profiling in wheat genome. H3K4me3 and H3K27me3 profiles of each chromosome in wheat A, B and D genomes. Colors of tracks represent different treatments with two histone marks (light blue: WW_K4, yellow: DT_K4, dark blue: WW_K27, orange DT_K27, the bottom blue: gene density). Reads were normalized to input [log2 (IP/input)].

A similar genomic distribution of H3K27me3 IP in the comparison of WW and DT was also found. Approximately 70% of peaks were in distal intergenic regions, 20% to 22% were in promoter regions. I further identified peak-related genes that were in the gene body or close to the promoter regions [≤ 2kb upstream of transcription start site (TSS)]. Total gene numbers of both

marks in the regions were 53,616 in well-watered and 75,924 in drought (data not shown). Surprisingly, 25,000 more genes were identified in drought with H3K4me3 than in well-watered plant (Table 2). Among these 72,008 genes identified from DT_K4, 43% (31,115) of the genes were unique to the drought condition. Approximately 11.2% of 46,085 genes identified from WW_K4 were unique to well-watered condition (Figure 6). In contrast to H3K4me3, the numbers of genes identified from H3K27me3 IPs were relatively close in WW (18,408 genes) and DT (14,683 genes). 39.2% (7,219/18,408) of genes identified from WW_K27 were well-watered specific but only 23.8% (3,494/14,683) of genes identified from DT_K27 were drought specific (Figure 6).

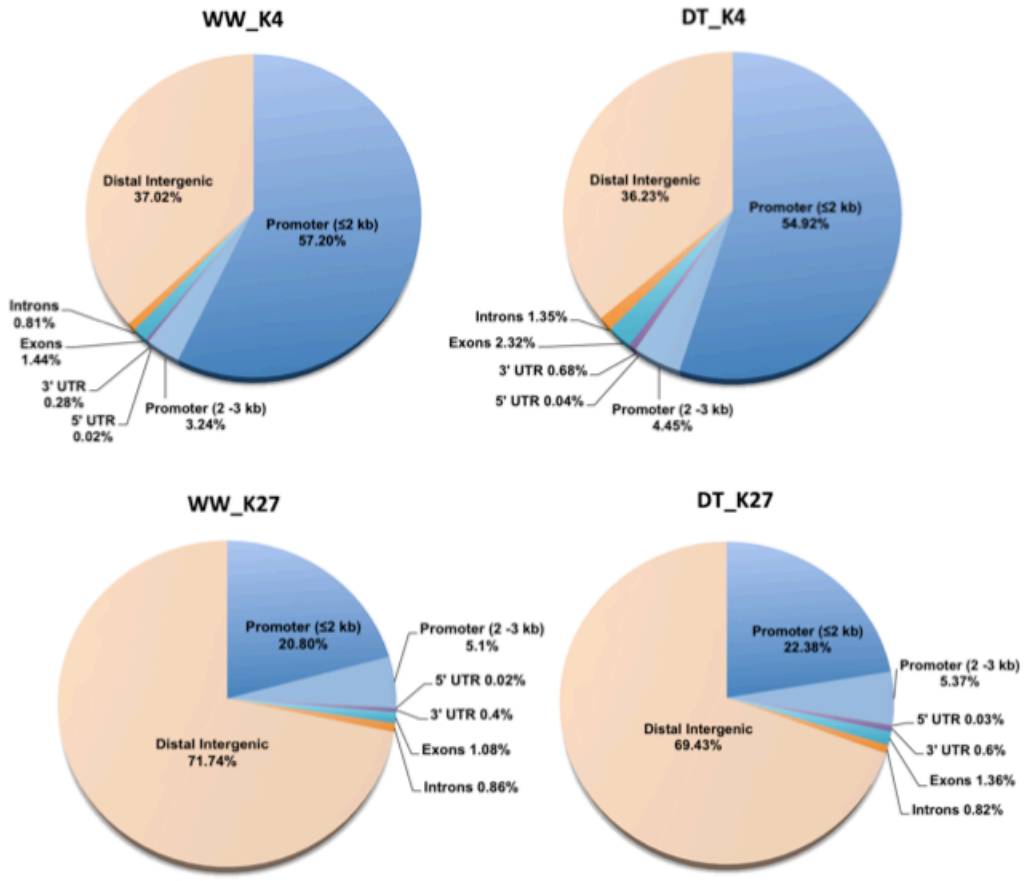

Figure 5. Peak distribution in well-watered and drought in wheat genome. Peaks identified from H3K4me3 and H3K27me3 marks related to genomic features.

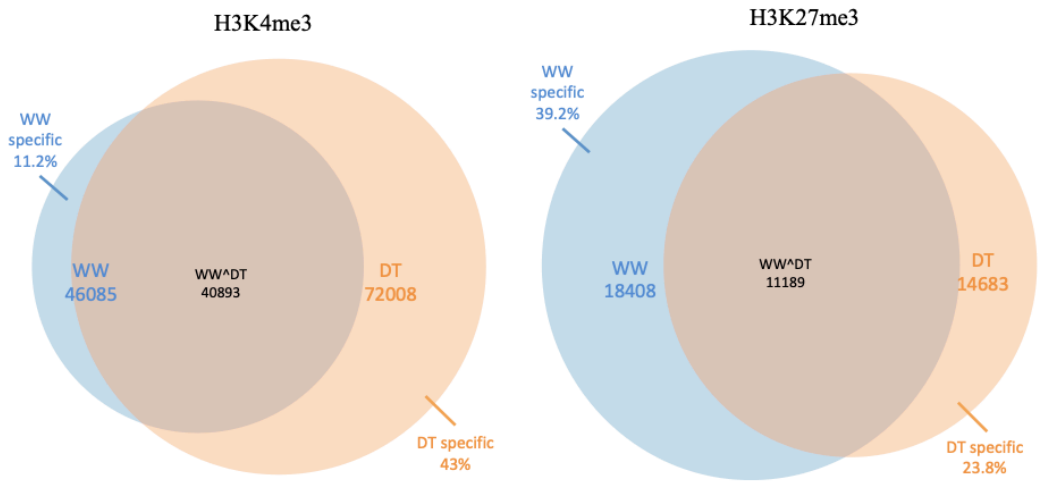

Figure 6. Total annotated genes from H3K4me3 and H3K27me3 modifications in well-watered and drought conditions. Left Venn graph shows total 46,085 H3K4me3 modified genes in well-watered (WW), 72,008 in drought (DT); 11.2% of them are WW-specific genes, 43% are DT-specific genes. Right Venn graph shows total 18,408 H3K27me3 modified genes in well-watered (WW), 14,683 in drought (DT); 39.2% of them are WW-specific genes, 23.8% are DT-specific genes.

3.5 Histone modification significantly enriched in drought responsive genes

To understand the relationship of histone modifications and peak-related genes, I further filtered the peak-related genes where peak enrichments are more significant than 2-fold change between drought and well-watered treatments. H3K4me3 mark was over two-fold enriched in 30,327 genes under drought-stress (Table 2) and about 56% (17,170 genes, data not shown) of H3K4me3 enriched genes in drought were drought specific. Gene ontology analysis on AgriGO (version 2.0, Tian et al., 2017) indicated that 17,170 drought-specific genes enriched with H3K4me3 were involved in intracellular organelles of cellular components (Table 3). Many of these genes were known to correspond to cell components in water deficit such as mitochondrial membrane (Zhang

et al., 2014), Rho GDP-dissociation inhibitor activity (Shen et al., 2017), autophagy (Bao et al., 2020), mitochondrial pyruvate transport, and glycerol-3-phosphate dehydrogenase (GPDH) which played an important role in lipid metabolism and maintaining redox potential in mitochondrial inner membrane (Zhao et al., 2018). In drought, 6,323 genes were significantly enriched with peaks of H3K27me3 marks (Table 2), and nearly 30% (1,857 genes, data not shown) of these genes were unique to drought (drought-specific genes). Among the drought-specific genes significantly enriched with H3K27me3, the extracellular region is the only significant hit in GO term category of cellular component. The genes identified were mainly related to cell wall biogenesis and xyloglucan metabolic process, which were known to be affected under drought stress (Iurlaro et al., 2016). These results suggested that water-deficit in wheat may change histone modifications not only in drought responsive genes that already had been modified under water-sufficient conditions but also in newly involved drought responsive genes in order to survive through dehydration stress.

Table 3 List of cellular components of H3K4me3 significantly enriched in drought unique genes

Cellular component	Gene numbers	p-value	FDR	GO term
Cytoplasm	626 (6.5%)	5.40E-10	6.10E-07	GO:0005737
Cell	1411 (14.6%)	3.90E-08	1.50E-05	GO:0005623
Cell part	1411 (14.6%)	3.90E-08	1.50E-05	GO:0044464
Intracellular	1354 (14.0%)	7.00E-08	2.00E-05	GO:0005622
Cytoplasmic part	455 (4.7%)	9.10E-08	2.10E-05	GO:0044444
Intracellular part	1255(13.0%)	6.70E-07	0.00013	GO:0044424
Intracellular organelle	893 (9.2%)	5.90E-06	0.00084	GO:0043229
Organelle	893 (9.2%)	5.90E-06	0.00084	GO:0043226
Organelle membrane	82 (0.8%)	8.70E-05	0.011	GO:0031090
Intracellular membrane-bounded organelle	617 (6.4%)	0.00011	0.012	GO:0043231
Membrane-bounded organelle	617 (6.4%)	0.00011	0.012	GO:0043227
Mitochondrial membrane	44 (0.5%)	0.00038	0.036	GO:0031966

3.6 Bivalent H3K4me3-H3K27me3 modification associated genes in drought

The coexistence of H3K4me3 (active) and H3K27me3 (repressive) marks has been proved to increase on stress-responsive genes under stress conditions (Zeng et al., 2019). I therefore investigated whether bivalency was involved upon drought stress. The peaks in the gene body and in promoter regions (≤ 2kb upstream of TSS) were first isolated. The "bivalent domain" is defined as the peak where H3K4me3 and H3K27me3 marks overlap over 1kb (Court et al., 2017). In total, 4,079 genes were determined as bivalent genes from both conditions. 2,204 bivalent genes were found in well-watered wheat, and 3,819 bivalent genes were found in drought-treatment wheat, and 1,079 bivalent genes were correlated to both well-watered and drought treatments (WW^DT, Figure 7). Overall, the percentage of bivalent genes in each treatment of total well-watered genes was 4.11% and was 5.03% of total drought-induced genes. These data indicate that the bivalent marks are enriched in drought-stressed wheat by over 1,600 genes.

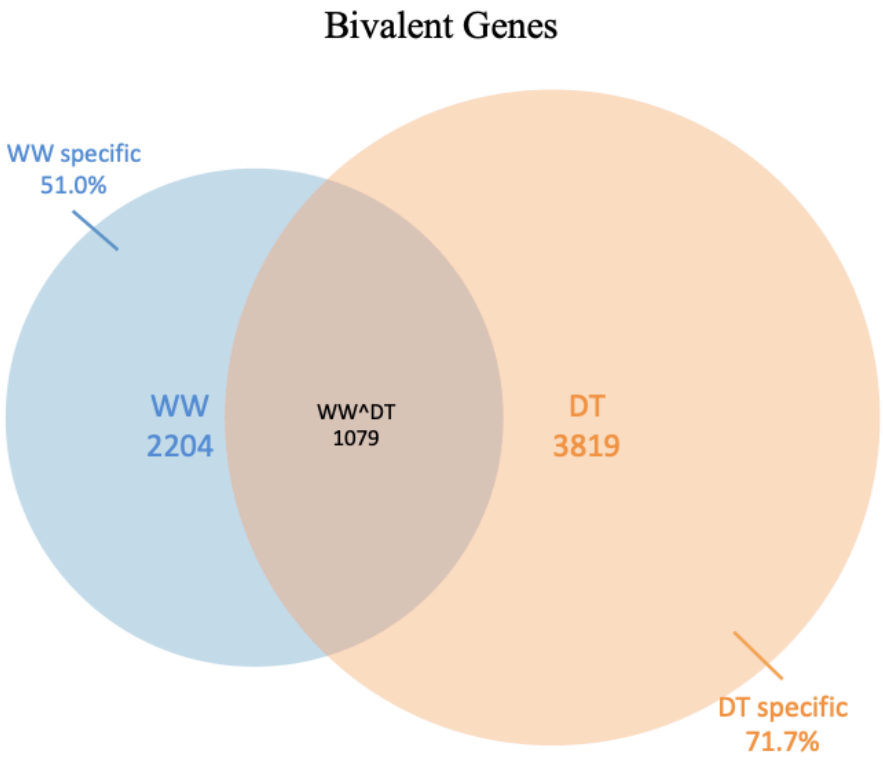

Figure 7. Number of bivalent genes identified in each condition. Bivalent genes identified of which total 2,204 genes from well-watered (WW) and total 3,819 genes from drought (DT) and 1,079 genes were present in both well-watered and drought conditions (WW^DT).

Comparing the histone bivalency of well-watered condition to drought-specific bivalent genes (71.7% in Figure 7) uncovers the regulation strategies plants reacted from normal condition to unfavorable condition. The GO term analysis showed that 18 biological processes identified from 2,204 bivalent genes in well-watered plant were involved in several metabolic processes, such as amino acid and fatty acid biosynthetic processes, which can be seen as general metabolisms under water-sufficient condition (Figure 8a). By contrast, 14 biological processes identified from 2,740 (71.7%) bivalent genes, which only present in drought, were further prone to cell wall biogenesis and phosphate ion transport processes (Figure 8b).

a

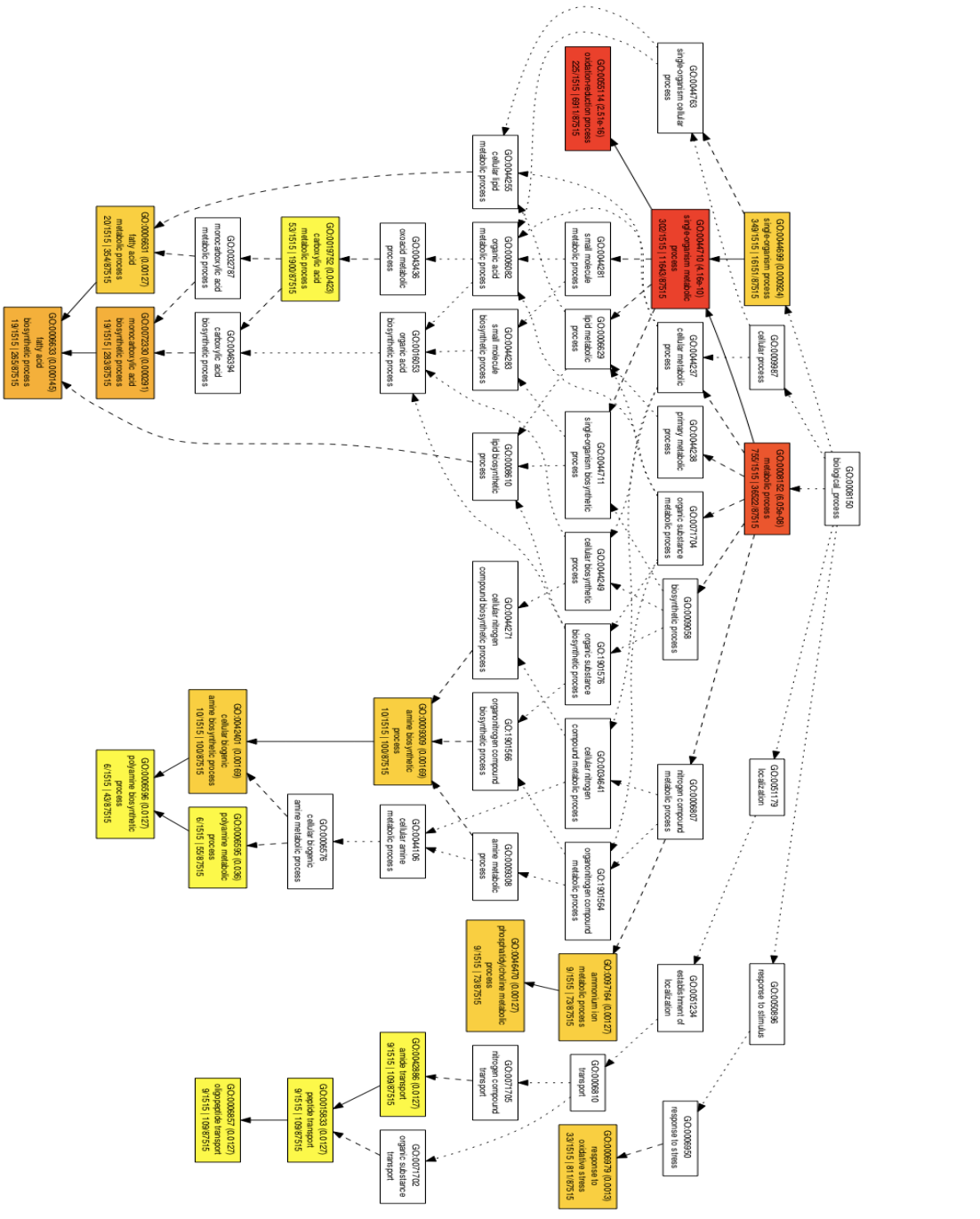
GO:0044699 (0.00024)
single-organism process
349/1515 | 16151/87515
GO:0044710 (4.16e-10)
single-organism metabolic process
332/1515 | 14643/87515
GO:0044763
single-organism cellular process
GO:0055114 (2.51e-16)
oxidation-reduction process
225/1515 | 6911/87515
GO:0009987
cellular process
GO:0008150
biological_process
GO:0008152 (6.05e-08)
metabolic process
755/1515 | 36622/87515
GO:0044281
small molecule metabolic process
GO:0006629
lipid metabolic process
GO:0044237
cellular metabolic process
GO:0044238
primary metabolic process
GO:0071704
organic substance metabolic process
GO:0044711
single-organism biosynthetic process
GO:0044249
cellular biosynthetic process
GO:0009058
biosynthetic process
GO:1901576
organic substance biosynthetic process
GO:0034641
cellular nitrogen compound metabolic process
GO:0006807
nitrogen compound metabolic process
GO:1901564
organonitrogen compound metabolic process
GO:0044271
cellular nitrogen compound biosynthetic process
GO:1901566
organonitrogen compound biosynthetic process
GO:0044106
cellular amine metabolic process
GO:0006576
cellular biogenic amine metabolic process
GO:0006596 (0.036)
polyamine metabolic process
6/1515 | 56/87515
GO:0006596 (0.0127)
polyamine biosynthetic process
6/1515 | 43/87515
GO:0042401 (0.00169)
cellular biogenic amine biosynthetic process
10/1515 | 100/87515
GO:0009309 (0.00169)
amine biosynthetic process
10/1515 | 100/87515
GO:0008610
lipid biosynthetic process
GO:0006082
organic acid metabolic process
GO:0044283
small molecule biosynthetic process
GO:0016053
organic acid biosynthetic process
GO:0046394
carboxylic acid biosynthetic process
GO:0032787
monocarboxylic acid metabolic process
GO:0072330 (0.00291)
monocarboxylic acid biosynthetic process
19/1515 | 283/87515
GO:0006631 (0.0127)
fatty acid metabolic process
20/1515 | 354/87515
GO:0006633 (0.00145)
fatty acid biosynthetic process
19/1515 | 265/87515
GO:0019752 (0.0423)
carboxylic acid metabolic process
53/1515 | 1900/87515
GO:0043436
oxoacid metabolic process
GO:0051179
localization
GO:0051234
establishment of localization
GO:0006810
transport
GO:0071705
nitrogen compound transport
GO:0015833 (0.0127)
peptide transport
9/1515 | 109/87515
GO:0006857 (0.0127)
oligopeptide transport
9/1515 | 109/87515
GO:0042886 (0.0127)
amide transport
9/1515 | 109/87515
GO:0006979 (0.0013)
response to oxidative stress
33/1515 | 81/87515
GO:0006950
response to stress
GO:0009896
response to stimulus
GO:0071702
organic substance transport
GO:0046470 (0.00127)
phosphatidylcholine metabolic process
9/1515 | 79/87515
GO:1097164 (0.00127)
ammonium ion metabolic process
9/1515 | 79/87515
Level9
Level8
Level7
Level6
Level5
Level4
Level3
Level2
Level1
is_a
one significant node

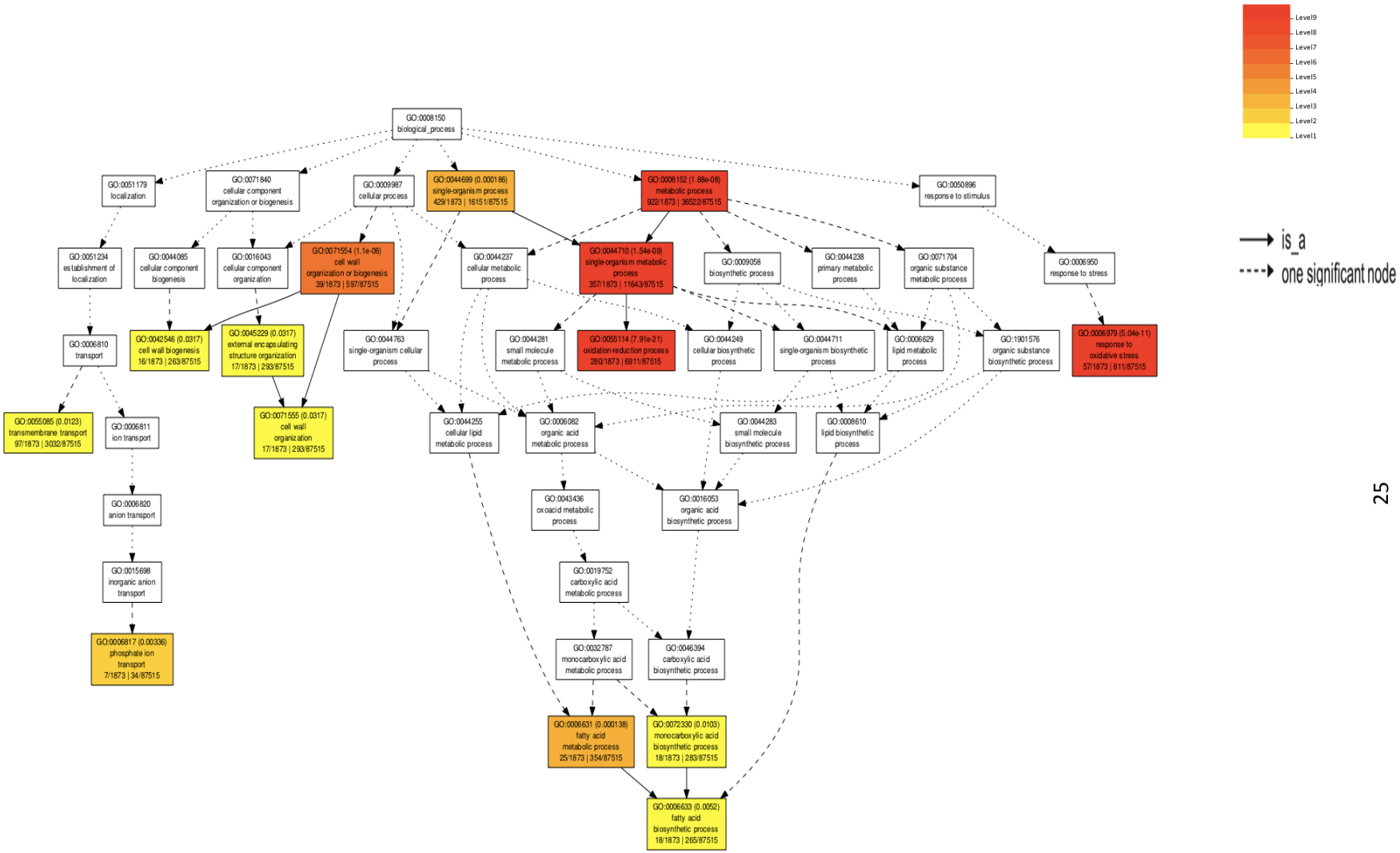
Level9
Level8
Level7
Level6
Level5
Level4
Level3
Level2
Level1
is_a
one significant node
GO:0008150 biological_process
GO:0051179 localization
GO:0071840 cellular component organization or biogenesis
GO:0009987 cellular process
GO:0044699 (0.000186) single-organism process 429/1873 | 16151/87515
GO:0008152 (1.88e-08) metabolic process 922/1873 | 36522/87515
GO:0050896 response to stimulus
GO:0051234 establishment of localization
GO:0044085 cellular component biogenesis
GO:0016043 cellular component organization
GO:0071554 (1.1e-06) cell wall organization or biogenesis 39/1873 | 597/87515
GO:0044237 cellular metabolic process
GO:0044710 (1.54e-09) single-organism metabolic process 357/1873 | 11643/87515
GO:0009058 biosynthetic process
GO:0044238 primary metabolic process
GO:0071704 organic substance metabolic process
GO:0006950 response to stress
GO:0006810 transport
GO:0042546 (0.0317) cell wall biogenesis 16/1873 | 263/87515
GO:0045229 (0.0317) external encapsulating structure organization 17/1873 | 293/87515
GO:0044763 single-organism cellular process
GO:0044281 small molecule metabolic process
GO:0055114 (7.91e-21) oxidation-reduction process 280/1873 | 6911/87515
GO:0044249 cellular biosynthetic process
GO:0044711 single-organism biosynthetic process
GO:0006629 lipid metabolic process
GO:1901576 organic substance biosynthetic process
GO:0006979 (5.04e-11) response to oxidative stress 57/1873 | 811/87515
GO:0055085 (0.0123) transmembrane transport 97/1873 | 3032/87515
GO:0006811 ion transport
GO:0071555 (0.0317) cell wall organization 17/1873 | 293/87515
GO:0044255 cellular lipid metabolic process
GO:0006082 organic acid metabolic process
GO:0044283 small molecule biosynthetic process
GO:0008610 lipid biosynthetic process
GO:0006820 anion transport
GO:0043436 oxoacid metabolic process
GO:0016053 organic acid biosynthetic process
GO:0015698 inorganic anion transport
GO:0019752 carboxylic acid metabolic process
GO:0006817 (0.00336) phosphate ion transport 7/1873 | 34/87515
GO:0032787 monocarboxylic acid metabolic process
GO:0046394 carboxylic acid biosynthetic process
GO:0006631 (0.000138) fatty acid metabolic process 25/1873 | 354/87515
GO:0072330 (0.0103) monocarboxylic acid biosynthetic process 18/1873 | 283/87515
GO:0006633 (0.0052) fatty acid biosynthetic process 18/1873 | 265/87515

Figure 8. Hieratical graph of biological process of bivalent genes. GO analysis from 2,204 well-watered bivalent genes (a) and 2,740 drought specific bivalent genes (b). Inside the box labeled by GO term, adjusted p-value, GO description. The degree of color is corresponding to the adjusted p-value, only statistically significant terms (FDR < 0.05) were colored.

3.7 Histone bivalency changed during drought stress

When plants encounter abiotic stress, immediate responses are required for plants to adjust their physiological functions to handle the environmental cue. In this study, the escalation of bivalency under drought treatment was observed, thus I hypothesized that plants rapidly alter physiological functions to adapt to dehydration stress by developing bivalent marks. The distribution and dynamic change of drought-induced bivalent marks in WW^DT and drought specific bivalent genes reveal the development of bivalency under the drought environment. I compared the features of histone modifications for the distinct genes from WW^DT or drought specific bivalent genes in the same GO terms identified. Noticeably, in one of the biological processes, fatty acid biosynthetic process (GO:0006633), 11 out of 18 drought specific bivalent genes contained significantly enriched or decreased (log2 fold change ≥ 1 or ≤ -1) peaks in H3K4me3 or H3K27me3 under drought-stress.

Table 4 GO:0006633 fatty acid biosynthetic process

Gene ID	H3K4me3	H3K27me3
DT-specific bivalent		
TraesCS1B02G052800	↑	↓
TraesCS1D02G042300	↑	↓
TraesCS1D02G401000	-	↓
TraesCS3B02G488500	↑	↓
TraesCS4A02G456600	↑	↑
TraesCS4B02G297500	↑	↑
TraesCS4D02G008100	-	↓
TraesCS4D02G296400	-	↓
TraesCS5B02G309800	↑	↓
TraesCS5D02G316100	-	↓
TraesCS6A02G415500	↑↓	↑↓
TraesCS6B02G324200	-	↓
TraesCS7A02G032900	↑	↑
TraesCS7A02G532300	↑	↑
TraesCS7B02G449300	-	↑↓
TraesCS7D02G029500	-	-
TraesCS7D02G101900	↑	-
TraesCS7D02G519400	-	↓
WW^DT-bivalent		
TraesCS1A02G039800	↓	-
TraesCS1A02G040900	↓	↓
TraesCS1A02G439000	-	-
TraesCS1D02G042100	↓	↓
TraesCS2A02G014600	-	-
TraesCS4A02G303900	↓	-
TraesCS5A02G309100	-	-
TraesCS5A02G309200	↓	-
TraesCS6A02G026800	↓	↓
TraesCS7A02G532100	-	-
TraesCS7B02G449000	↓	-
TraesCS7D02G076400	↑	↑
TraesCS7D02G089200	↓	-

*Peak fold change was normalized to well-watered value. (↑: log2 ≥ 1, ↓: log2 ≤ -1, - : no enrichment)

The bivalency of these drought specific bivalent genes was not yet established until they encountered the drought stress. The bivalency occurred by reducing the repressive marks and

obtaining the active marks from the original chromatin state. By contrast, though both H3K4me3 and H3K27me modifications slightly decreased in WW^DT bivalent genes upon dehydration, the bivalency was preserved during drought stress (Table 4). Visualized bivalent features of selected genes were presented in Figure 9.

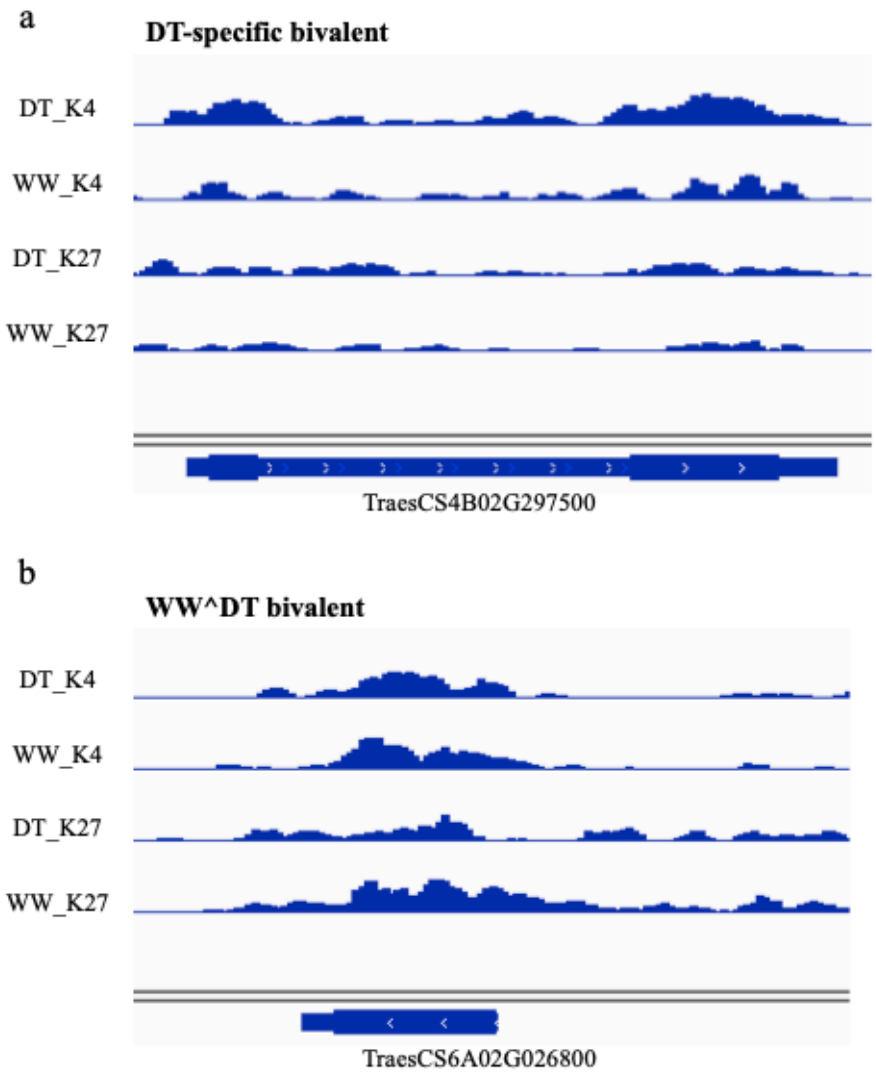

Figure 9. Selected bivalent genes visualized in IGV.

Peaks significantly enriched in H3K4me3 and decreased in H3K27me3 under water deficit in DT-specific bivalent gene, TraesCS4B02G297500 (a). H3K4me3 and H3K27me3 modifications decreased in WW^DT specific gene, TraesCS6A02G026800 (b). Bivalency is defined by ≥ 1kb peak overlapped

with H3K4me3 and H3K27me3. (DT_K4: drought H3K4me3 ChIP, WW_K4: well-watered H3K4me3 ChIP, DT_K27: drought H3K27me3 ChIP, WW_K27: well-watered H3K27me3 ChIP)

These results suggested that plants dynamically established bivalency while retaining the existed bivalency in response to drought stress. The histones of drought specific genes were modified after the occurrence of water deficit. Previous study indicated that the accumulation of H3K27me3 did not interfere the activations of dehydration stress-responding genes by H3K4me3 (Liu et al., 2014). I then isolated the genes that were drought specific and bivalent simultaneously to identify the most crucial drought-responsive genes under drought stress. GO term analysis showed that cross related genes of drought-specific and bivalent involved in oxidation-reduction biological process and iron ion binding, heme-binding, etc. for molecular function (Table 5), which were known to be related to nitric oxide and oxidative stress caused by water deficit (Marondedze et al., 2019; Gupta et al., 2011).

Table 5 List of molecular function of drought-specific gene with histone bivalency

Molecular function	Gene numbers	p-value	FDR	GO term
Oxidoreductase activity, acting on paired donors, with incorporation or reduction of molecular oxygen	12 (17.6%)	2.10E-06	0.00018	GO:0016705
Iron ion binding	12 (17.6%)	1.60E-06	0.00018	GO:0005506
Heme binding	12 (17.6%)	2.40E-05	0.0011	GO:0020037
Tetrapyrrole binding	12 (17.6%)	2.60E-05	0.0011	GO:0046906
Oxidoreductase activity	20 (29.6%)	4.50E-05	0.0015	GO:0016491

CHAPTER IV

DISCUSSION

4.1 Overall histone modifications in wheat

Histone modifications of H3K4me3 and H3K27me3 were well-known to regulate gene expression in plants in order to adapt abiotic stress. H3K4me3 is positively correlated with active gene whereas H4K27me3 is negatively correlated with gene activation. Here I use the ChIP-seq approach to identify the first genome-wide map of chromatin patterns in drought-stressed winter wheat and to examine whether the both marks are associated with winter wheat response to drought stress. The H3K4me3 mark primarily occurred in interstitial and distal end regions of chromosomes, and H3K27me3 modifications were majorly localized to the end regions in chromosomes, which was similar to previous studies (Qi et al., 2018; Li et al., 2019). The percentages of mapped reads to the reference genome are similar among well-watered and drought plants. In addition, peak distributions of H3K4me3 and H3K27me3 marks also showed a similar proportion of wheat genome regions in well-watered and drought-stressed plants. This indicates that the proportion of histone modification distributed in different genome regions was not altered after drought stress in wheat. In previous studies, histone distributions varied in stress responsive genes by different transcript levels (Zong et al., 2013; Zeng et al., 2019). Therefore, analyzing gene expression along with histone modification may reveal a different pattern of histone distribution in genome regions.

4.2 Roles of H3K4me3 and H3K27me3 in gene regulations

Although the peaks of histone mark distributions in genome regions were similar in well-watered and drought treatments, a slight increase of exon H3K4me3 deposition was observed after drought treatment (Figure 5). Studies in several organisms have shown that gradually increased H3K4me3 levels on coding regions is associated with RNA polymerase II elongation efficiency (Gerber and Shilatifard, 2003; Kim et al., 2008; Pu et al., 2018). The regulatory function of the link between H3K4me3 mark and transcriptional elongation on drought-responsive genes however is not well understood. Total genes annotated from H3K4me3 were also observed dramatically increased under dehydration stress. This can be seen with the increasing number of peaks in drought. In this study, the peaks of 30,327 genes were significantly enriched and the peaks of 21,264 genes were significantly decreased after drought treatment (Table 2). Furthermore, the repressive mark, H3K27me3 modification, showed an opposite pattern of peak enrichment and decrease in drought responsive genes (Table 2). Similar to the pattern of significantly enriched active and decreased repressive histone modifications in our GO analysis results (data not shown), a significant number of enriched gene transcripts responded to carbohydare metabolism, hormone signal transduction, membrane lipid metabolism and nucleobase-containing compound were observed after drought treatment in Italian ryegrass (*Lolium multiflorum*; Pan et al., 2016). This observation implies that more drought responsive genes were activated by enhancing H3K4me3 modification or reducing H3K27me3 modification during drought stress. Interestingly, the GO term analysis showed phenylpropanoid metabolic process, lignin metabolic process and cell wall macromolecule metabolic process were highly related to H3K27me3 significantly decreased genes (data not shown). Lignin is known for its involvement of signaling pathway in strengthening cell wall to defense as an antioxidant during abiotic stress response, and possibly associated with phenylpropanoid pathway (Blokhina et al., 2003; Betz et al.,). This finding suggests that the role of decreased H3K27me3 modification in

up-regulating drought responsive genes may be as crucial as the active modification of H3K4me3.

4.3 Involvement of bivalent modifications

Bivalent modifications are located on poised promoters of developmental genes in embryonic stem cells, allowing for rapid activation upon developmental cues (Bernstein et al., 20016). Yet, it is still unclear whether the bivalent mark is involved in plants responding to environmental stimuli. Our analysis indicated that over 96% of bivalent domains were enriched in promoter regions. I further evaluated the bivalent genes with RNA-sequencing dataset generated in our previous drought study and found that 7% (12/165) of differential expressed genes (DEGs, up- or down-regulated in drought treatment, fold change ≥ 4) displayed bivalent enrichment. The bivalent genes often carry both the H3K4me3 and H3K27me3 modifications at promoter regions and typically keep low-level gene expression (Thalheim et al., 2017), the less stringent fold-change cutoff of transcribed genes may be applied in analysis. Not including the biological processes present in well-watered condition, the bivalent genes of drought treatment also showed the relationship to cell wall biogenesis and phosphate ion transport processes. Genes involved in cell wall cellular components such as xyloglucosyl transferase/hydrolase is known to improve severe drought tolerance in Arabidopsis and tomato (Cho et al., 2016; Choi et al., 2011). In addition, pectinesterases have known to be involved in cell wall remodeling and are important for controlling water loss by regulating stomatal function under various abiotic stresses (Amsbury et al., 2016; Le Gall et al., 2015). Phosphate transporters are important for maintaining the phosphorous (Pi) distribution in plants, which is a crucial element in various metabolic processes of protein biogenesis under drought stress (Bohnert et al., 1998). Furthermore, under Pi starvation, nucleosome occupancy and colocalization of H3K4me3 and H2A.Z at TSS are correlated with expression of Pi-deficiency response genes that target cell wall structure in rice (Foroozani et al., 2020). Though a similar enrichment of bivalent marks were observed through

the bivalent genes in cold-stressed potato, the expression levels of those genes varied significantly, of which over 78% of bivalent genes were significantly up- or down-regulated and 20 % were maintained at same levels (Zeng et al., 2019). Our finding indicated that 71.1% of drought bivalent modifications were developed upon the drought treatment whereas 18.9% of the bivalency unchanged on the genes which were common in well-watered and drought treatments; however, direct evidence related to gene expression has not yet been proven in this study. Therefore, exploring the association of transcription levels and these drought-specific bivalent genes is required. Further comparison of bivalent histone modifications and gene transcriptions are important for proving bivalent switch on/off function, which active and repressive marks function independently but are not mutually exclusive.

REFERENCES

Agarwal PK, Agarwal P, Reddy MK, Sopory SK (2006) Role of DREB transcription factors in abiotic and biotic stress tolerance in plants. Plant Cell Rep 25:1263-1274

Allfrey VG, Faulkner R, Mirsky AE (1964) Acetylation and methylation of histones and their possible role in the regulation of RNA synthesis. Proc Natl Acad Sci51:786-794

Amsbury S, Hunt L, Elhaddad N, Baillie A, Lundgren M, Verhertbruggen Y, Scheller HV, Knox JP, Fleming AJ, Gray JE (2016) Stomatal function requires dectin De-methyl-esterification of the guard cell wall. Curr Biol 26:2899-2906

Bao Y, Song W-M, Wang P, Yu X, Li B, Jiang C, Shiu S-H, Zhang H, Bassham DC (2020) COST1 regulates autophagy to control plant drought tolerance. Proc Natl Acad Sci 117:7482-7493

Basenko EY, Sasaki T, Ji L, Prybol CJ, Burckhardt RM, Schmitz RJ, Lewis ZA (2015) Genome-wide redistribution of H3K27me3 is linked to genotoxic stress and defective growth. Proc Natl Acad Sci 112:E6339-6348

Bäurle I, Trindade I (2020) Chromatin regulation of somatic abiotic stress memory. J Exp Bot eraa098

Bernstein BE, Kamal M, Lindblad-Toh K, Bekiranov S, Bailey DK, Huebert DJ, McMahon S, Karlsson EK, Kulbokas EJ, Gingeras TR, Schreiber SL, Lander ES (2005) Genomic maps and comparative analysis of histone modifications in human and mouse. Cell 120:169-181

Bernstein BE, Mikkelsen TS, Xie X, Kamal M, Huebert DJ, Cuff J, Fry B, Meissner A, Wernig M, Plath K, Jaenisch R, Wagschal A, Feil R, Schreiber SL, Lander ES (2006) A bivalent chromatin structure marks key developmental genes in embryonic stem cells. Cell 125:315-326

Betz GA, Gerstner E, Stich S, Winkler B, Welzl G, Kremmer E, Langebartels C, Heller W, Sandermann H, Ernst D (2009) Ozone affects shikimate pathway genes and secondary metabolites in saplings of European beech (*Fagus sylvatica* L.) grown under greenhouse conditions. Trees 23:539-553

Blokhina O, Virolainen E, Fagerstedt KV (2003) Antioxidants, oxidative damage and oxygen deprivation stress: a review. Ann Bot 91 Spec No:179-194

Bohnert HJ, Sheveleva E (1998) Plant stress adaptations- making metabolism move. Curr Opin Plant Biol 1:267-274

Cao R, Wang L, Wang H, Xia L, Erdjument-Bromage H, Tempst P, Jones RS, Zhang Y (2002) Role of histone H3 lysine 27 methylation in Polycomb-group silencing. Science 298:1039-1043

Cao S, Wang Y, Li Z, Shi W, Gao F, Zhou Y, Zhang G, Feng J (2019) Genome-wide identification and expression analyses of the chitinases under cold and osmotic stress in *Ammopiptanthus nanus*. Genes 10:472

Chilcott EC, Cole JS (1917) Growing winter wheat on the great plains. Farmers' Bulletin 895

Cho SK, Kim JE, Park JA, Eom TJ, Kim WT (2006) Constitutive expression of abiotic stress-inducible hot pepper CaXTH3, which encodes a xyloglucan endotransglucosylase/hydrolase homolog, improves drought and salt tolerance in transgenic Arabidopsis plants. FEBS Lett 580:3136-3144

Choi JY, Seo YS, Kim SJ, Kim WT, Shin JS (2011) Constitutive expression of CaXTH3, a hot pepper xyloglucan endotransglucosylase/hydrolase, enhanced tolerance to salt and drought stresses without phenotypic defects in tomato plants (*Solanum lycopersicum* cv. *Dotaerang*). Plant Cell Rep 30:867-877

Court F, Arnaud P (2017) An annotated list of bivalent chromatin regions in human ES cells: a new tool for cancer epigenetic research. Oncotarget 8:4110-4124

Cruz de Carvalho MH (2008) Drought stress and reactive oxygen species: Production, scavenging and signaling. Plant Signal Behav 3:156-165

Davey CA, Sargent DF, Luger K, Maeder AW, Richmond TJ (2002) Solvent mediated interactions in the structure of the nucleosome core particle at 1.9 Å resolution. J Mol Biol 319:1097-1113

David SA, Piégu B, Hennequet-Antier C, Pannetier M, Aguirre-Lavin T, Crochet S, Bordeau T, Couroussé N, Brionne A, Bigot Y, Collin A, Coustham V (2017) An assessment of fixed and native chromatin preparation methods to study histone post-translational modifications at a whole genome scale in skeletal muscle tissue. Biol Proced Online 19:10-10

Earl HJ (2003) A precise gravimetric metric method for simulating drought stress in pot experiments. Crop Sci 43:1868-1873

Fan X, Lamarre-Vincent N, Wang Q, Struhl K (2008) Extensive chromatin fragmentation improves enrichment of protein binding sites in chromatin immunoprecipitation experiments. Nucleic Acids Res 36:e125-e125

Farooq M, Wahid A, Kobayashi N, Fujita D, Basra SMA (2009) Plant drought stress: effects, mechanisms and management. Agron Sustain Dev 29:185-212

Foroozani M, Zahraeifard S, Oh D-H, Wang G, Dassanayake M, Smith AP (2020) Low-phosphate chromatin dynamics predict a cell wall remodeling network in rice shoots. Plant Physiol 182:1494-1509

Fowler D (2018) Growth stages of wheat. Winter wheat production manual. Chapter 10. Ducks Unlimited Canada and Conservation Production Systems Ltd

Gendrel AV, Lippman Z, Martienssen R, Colot V (2005) Profiling histone modification patterns in plants using genomic tiling microarrays. Nat Methods 2:213-218

Gerber M, Shilatifard A (2003) Transcriptional elongation by RNA polymerase II and histone methylation. J Biol Chem 278:26303-26306

Grover A (2012) Plant Chitinases: Genetic Diversity and Physiological Roles. Crit Rev Plant Sci 31:57-73

Gupta KJ, Hebelstrup KH, Mur LAJ, Igamberdiev AU (2011) Plant hemoglobins: Important players at the crossroads between oxygen and nitric oxide. FEBS Letters 585:3843-3849

Haring M, Offermann S, Danker T, Horst I, Peterhansel C, Stam M (2007) Chromatin immunoprecipitation: optimization, quantitative analysis and data normalization. Plant Methods 3:11-11

Hu Y, Zhang L, Zhao L, Li J, He S, Zhou K, Yang F, Huang M, Jiang L, Li L (2011) Trichostatin A selectively suppresses the cold-induced transcription of the ZmDREB1 gene in maize. PLoS ONE 6:e22132-e22132

Iurlaro A, De Caroli M, Sabella E, De Pascali M, Rampino P, De Bellis L, Perrotta C, Dalessandro G, Piro G, Fry SC, Lenucci MS (2016) Drought and heat differentially affect XTH expression and XET activity and action in 3-day-old seedlings of durum wheat cultivars with different stress susceptibility. Front Plant Sci 7:1686-1686

Johnson DS, Mortazavi A, Myers RM, Wold B (2007) Genome-wide mapping of in vivo protein-DNA interactions. Science 316:1497-1502

Kim J-M, To TK, Nishioka T, Seki M (2010) Chromatin regulation functions in plant abiotic stress responses. Plant Cell Environ 33:604-611

Kim JM, To TK, Ishida J, Morosawa T, Kawashima M, Matsui A, Toyoda T, Kimura H, Shinozaki K, Seki M (2008) Alterations of lysine modifications on the histone H3 N-tail under drought stress conditions in Arabidopsis thaliana. Plant Cell Physiol 49:1580-1588

Kouzarides T (2007) Chromatin modifications and their function. Cell 128:693-705

Le Gall H, Philippe F, Domon JM, Gillet F, Pelloux J, Rayon C (2015) Cell wall metabolism in response to abiotic stress. Plants (Basel) 4:112-166

Li H, Yan S, Zhao L, Tan J, Zhang Q, Gao F, Wang P, Hou H, Li L (2014) Histone acetylation associated up-regulation of the cell wall related genes is involved in salt stress induced maize root swelling. BMC Plant Biol 14:105

Li Z, Wang M, Lin K, Xie Y, Guo J, Ye L, Zhuang Y, Teng W, Ran X, Tong Y, Xue Y, Zhang W, Zhang Y (2019) The bread wheat epigenomic map reveals distinct chromatin architectural and evolutionary features of functional genetic elements. Genome Biol 20:139

Lisar SY, Bakhshayeshan-Agdam H (2016) Drought Stress in Plants: Causes, Consequences, and Tolerance. Drought Stress Tolerance in Plants, Vol 1. Springer International Publishing Switzerland. 1: 1-16

Liu N, Fromm M, Avramova Z (2014) H3K27me3 and H3K4me3 chromatin environment at super-induced dehydration stress memory genes of *Arabidopsis thaliana*. Mol Plant 7:502-513

Lugojan C, Ciulca S (2011) Evaluation of relative water content in winter wheat. J Hortic For Biotech 15:173-177

Mafakheri A, Siosemardeh A, Bahramnejad B, Struik PC, Sohrabi Y (2010) Effect of drought stress on yield, proline and chlorophyll contents in three chickpea cultivars. Aust J Crop Sci 8:580-585

Marburger D, Calhoun R, Hunger B, Watson B, Gillespie C (2018) Oklahoma Small Grains Variety Performance Tests 2017-2018. Oklahoma State University

Marondedze C, Thomas L, Gehring C, Lilley KS (2019) Changes in the Arabidopsis RNA-binding proteome reveal novel stress response mechanisms. BMC plant biol 19:139-139

Michaletti A, Naghavi MR, Toorchi M, Zolla L, Rinalducci S (2018) Metabolomics and proteomics reveal drought stress responses of leaf tissues from spring wheat. Sci Rep 8:5710

Miller MJ, Scalf M, Rytz TC, Hubler SL, Smith LM, Vierstra RD (2013) Quantitative proteomics reveals factors regulating RNA biology as dynamic targets of stress-induced SUMOylation in Arabidopsis. Mol Cell Proteomics 12:449-463

Okitsu CY, Hsieh JCF, Hsieh CL (2010) Transcriptional activity affects the H3K4me3 level and distribution in the coding region. Mol Cell Biol 30:2933

Pan L, Zhang X, Wang J, Ma X, Zhou M, Huang L, Nie G, Wang P, Yang Z, Li J (2016) Transcriptional profiles of drought-related genes in modulating metabolic processes and antioxidant defenses in *Lolium multiflorum*. Front Plant Sci 7:519-519

Park PJ (2009) ChIP–seq: advantages and challenges of a maturing technology. Nat Rev Genet 10:669-680

Pfluger J, Wagner D (2007) Histone modifications and dynamic regulation of genome accessibility in plants. Curr Opin Plant Biol 10:645-652

Pu M, Wang M, Wang W, Velayudhan SS, Lee SS (2018) Unique patterns of trimethylation of histone H3 lysine 4 are prone to changes during aging in Caenorhabditis elegans somatic cells. PLOS Genetics 14:e1007466

Qi M, Li Z, Liu C, Hu W, Ye L, Xie Y, Zhuang Y, Zhao F, Teng W, Zheng Q, Fan Z, Xu L, Lang Z, Tong Y, Zhang Y (2018) CGT-seq: epigenome-guided de novo assembly of the core genome for divergent populations with large genome. Nucleic Acids Res 46:e107

Ramírez F, Ryan DP, Grüning B, Bhardwaj V, Kilpert F, Richter AS, Heyne S, Dündar F, Manke T (2016) deepTools2: a next generation web server for deep-sequencing data analysis. Nucleic Acids Res 44:W160-W165

Ren B, Robert F, Wyrick JJ, Aparicio O, Jennings EG, Simon I, Zeitlinger J, Schreiber J, Hannett N, Kanin E, Volkert TL, Wilson CJ, Bell SP, Young RA (2000) Genome-wide location and function of DNA binding proteins. Science 290:2306-2309

Roy D, Paul A, Roy A, Ghosh R, Ganguly P, Chaudhuri S (2014) Differential acetylation of histone H3 at the regulatory region of OsDREB1b promoter facilitates chromatin remodelling and transcription activation during cold stress. PLoS ONE 9:e100343

Sade D, Sade N, Shriki O, Lerner S, Gebremedhin A, Karavani A, Brotman Y, Osorio S, Fernie AR, Willmitzer L, Czosnek H, Moshelion M (2014) Water balance, hormone homeostasis, and sugar signaling are all involved in tomato resistance to tomato yellow leaf curl virus. Plant Physiol 165:1684-1697

Samarah NH (2005) Effects of drought stress on growth and yield of barley. Agron Sustain Dev 25:145-149

Samarah NH, Alqudah AM, Amayreh JA, McAndrews GM (2009) The effect of late-terminal drought stress on yield components of four barley cultivars. J Agron Crop Sci 195:427-441

Shen J-L, Li C-L, Wang M, He L-L, Lin M-Y, Chen D-H, Zhang W (2017) Mitochondrial pyruvate carrier 1 mediates abscisic acid-regulated stomatal closure and the drought response by affecting cellular pyruvate content in Arabidopsis thaliana. BMC Plant Biol 17:217

Siddique MRB, Hamid A, Islam MS (2000) Drought stress effects on water relations of wheat. Botanical Bulletin of Academia Sinica 41:35-39

Somero GN (1992) Adapting to Water stress: convergence on common solutions. Water and Life:3-18

Thalheim T, Herberg M, Loeffler M, Galle J (2017) The Regulatory Capacity of Bivalent Genes-A Theoretical Approach. Int J Mol Sci 18:1069

Thorvaldsdóttir H, Robinson JT, Mesirov JP (2013) Integrative Genomics Viewer (IGV): high-performance genomics data visualization and exploration. Brief Bioinform 14:178-192

Tian T, Liu Y, Yan H, You Q, Yi X, Du Z, Xu W, Su Z (2017) AgriGO v2.0: a GO analysis toolkit for the agricultural community, 2017 update. Nucleic Acids Res 45:W122-W129

USDA-NASS (2019) Crop Production (wheat). Oklahoma Crop Reports

van Dijk K, Ding Y, Malkaram S, Riethoven JJ, Liu R, Yang J, Laczko P, Chen H, Xia Y, Ladunga I, Avramova Z, Fromm M (2010) Dynamic changes in genome-wide histone H3 lysine 4 methylation patterns in response to dehydration stress in *Arabidopsis thaliana*. BMC Plant Biol 10:238

Verbsky ML, Richards EJ (2001) Chromatin remodeling in plants. Curr Opin Plant Biol 4:494-500

Verslues PE, Agarwal M, Katiyar-Agarwal S, Zhu J, Zhu JK (2006) Methods and concepts in quantifying resistance to drought, salt and freezing, abiotic stresses that affect plant water status. Plant J 45:523-539

Voigt P, Tee W-W, Reinberg D (2013) A double take on bivalent promoters. Genes Dev 27:1318-1338

Wardlaw IF, Willenbrink J (2000) Mobilization of fructan reserves and changes in enzyme activities in wheat stems correlate with water stress during kernel filling. New Phytol 148:413-422

Wedel C, Siegel TN (2017) Genome-wide analysis of chromatin structures in *Trypanosoma brucei* using high-resolution MNase-ChIP-seq. Exp Parasitol 180:2-12

Wu J, Grunstein M (2000) 25 years after the nucleosome model: chromatin modifications. Trends Biochem Sci 25:619-623

Wu JQ, Snyder M (2008) RNA polymerase II stalling: loading at the start prepares genes for a sprint. Genome biology 9:220-220

Yu G, Wang LG, He QY (2015) ChIPseeker: an R/Bioconductor package for ChIP peak annotation, comparison and visualization. Bioinformatics 31:2382-2383

Zeng Z, Zhang W, Marand AP, Zhu B, Buell CR, Jiang J (2019) Cold stress induces enhanced chromatin accessibility and bivalent histone modifications H3K4me3 and H3K27me3 of active genes in potato. Genome Biol 20:123

Zhang B, Van Aken O, Thatcher L, De Clercq I, Duncan O, Law SR, Murcha MW, van der MerI M, Seifi HS, Carrie C, Cazzonelli C, Radomiljac J, Höfte M, Singh KB, Van Breusegem F, Whelan J (2014) The mitochondrial outer membrane AAA ATPase AtOM66 affects cell death and pathogen resistance in *Arabidopsis thaliana*. Plant J 80:709-727

Zhang X, Bernatavichute YV, Cokus S, Pellegrini M, Jacobsen SE (2009) Genome-wide analysis of mono-, di- and trimethylation of histone H3 lysine 4 in *Arabidopsis thaliana*. Genome Biol 10:R62

Zhang X, Clarenz O, Cokus S, Bernatavichute YV, Pellegrini M, Goodrich J, Jacobsen SE (2007) Whole-genome analysis of histone H3 lysine 27 trimethylation in Arabidopsis. PLOS Biol 5:e129

Zhang Y, Liu T, Meyer CA, Eeckhoute J, Johnson DS, Bernstein BE, Nusbaum C, Myers RM, Brown M, Li W, Liu XS (2008) Model-based analysis of ChIP-Seq (MACS). Genome Biol 9:R137

Zhao Y, Li X, Wang F, Zhao X, Gao Y, Zhao C, He L, Li Z, Xu J (2018) Glycerol-3-phosphate dehydrogenase (GPDH) gene family in *Zea mays L.*: Identification, subcellular localization, and transcriptional responses to abiotic stresses. PLoS ONE 13:e0200357

Zong W, Zhong X, You J, Xiong L (2013) Genome-wide profiling of histone H3K4-tri-methylation and gene expression in rice under drought stress. Plant Mol Biol 81:175-188

VITA

Chi-Ping Liao

Candidate for the Degree of

Master of Science

Thesis: GENOME-WIDE ANALYSIS OF HISTONE 3 LYSINE 4 AND HISTONE 3 LYSINE 27 TRIMETHYLATION MODIFICATIONS IN DROUGHT INDUCED WINTER WHEAT

Major Field: Biochemistry and Molecular Biology

Biographical:

Education:

Completed the requirements for the Master of Science in Biochemistry and Molecular Biology at Oklahoma State University, Stillwater, Oklahoma in July, 2020.

Completed the requirements for the Master of Science in Oral Biology at National Taiwan University, Taipei City, Taiwan in 2010.

Completed the requirements for the Bachelor of Science in Plant Pathology at National Chung-Hsing University, Taichung City, Taiwan in 2008.